

THE STUDY OF THE RADIAL LOCATION OF QUASI-COHERENT MODES BY HEAVY ION BEAM PROBE IN THE TJ-II STELLARATOR

Ph.O. Khabanov¹, L.G. Eliseev¹, N.K. Khartchev¹, C. Hidalgo², A.S. Kozachek³, L.I. Krupnik³, S.E. Lysenko¹, A.V. Melnikov^{1,4}, A.A. Chmyga³, G.N. Deshko³, S.M. Khrebtov³, A.D. Komarov³, A. Molinero², J.L. de Pablos² and TJ-II team²

¹*National Research Centre “Kurchatov Institute”, Moscow, Russia;*

²*Fusion National Laboratory, CIEMAT, Madrid, Spain;*

³*National Science Center Kharkov Institute of Physics and Technology, Institute of Plasma Physics, Kharkiv, Ukraine;*

⁴*National Research Nuclear University “MEPhI”, Moscow, Russia*

Recent experiments in low magnetic shear flexible heliac TJ-II have shown that steady frequency and chirping Alfvén Eigenmodes take place with $100 \text{ kHz} < f_{\text{AE}} < 300 \text{ kHz}$ at both pure NBI and combined ECR and NBI heated plasmas with low line-averaged density $\bar{n}_e = (0.3 \dots 1.5) \times 10^{19} \text{ m}^{-3}$ at Low Field Side (LFS) and High Field Side (HFS) of the plasma column. Furthermore, several types of low-frequency modes with $f < 30 \text{ kHz}$, such as suprathreshold electrostatic modes, tearing-like modes, quasicohherent modes with long-range potential correlations, were also observed. Power spectra for electrostatic and electromagnetic oscillations for all types of modes are presented along with their spatial location detected by dual Heavy Ion Beam Probe (HIBP).

PACS: 52.55.Hc, 52.35.-g, 52.35.Bj, 52.35.Ra

INTRODUCTION

Heavy Ion Beam Probe (HIBP) becomes recently an effective tool to study plasma potential and turbulence in toroidal fusion devices. This diagnostic was applied for the studies of Geodesic Acoustic Mode, MHD-tearing modes and quasicohherent modes in T-10 tokamak [1-3]. In the TJ-II stellarator an advanced dual HIBP, consisting of two toroidally separated HIBPs becomes an effective tool to study Alfvén Eigenmodes (AE) in NBI heated plasmas [4, 5].

The aim of the present study is to investigate the broadband plasma oscillations and to detect the spatial location for various types of modes observed in TJ-II: Alfvén eigenmodes, suprathreshold electron modes, tearing-like modes, modes with long-range potential correlations. The spatial HIBP scan passing from low-field side (LFS) via plasma center to high-field side (HFS) and back was used to detect the mode spatial locations. These data was supported by the data from the second HIBP that was either at the fixed spatial point or also scanned radially together with the data by Mirnov probe array and bolometer (AXUV) array.

1. EXPERIMENTAL SETUP

TJ-II is a four-period flexible heliac with low magnetic shear, and $B_0 = 0.95 \text{ T}$, $R_0 = 1.5 \text{ m}$, and $\langle a \rangle = 0.22 \text{ m}$. The experiments were performed in the standard magnetic configuration denoted 100_44_64. The numbers in this label refer to the currents in the magnetic field coils, ICC_IHX_IVF (see Fig. 1 in [6]) with vacuum rotational transform $t_{\text{vac}} = \sqrt{2}\pi$ increasing from $t_{\text{vac}}(0) = 1.55$ to 1.65. Here ICC is a current in the Circular Coil, IHX in the Helical Coil and IVF in the Vertical Field Coil in kA/10. The studies were performed in Hydrogen plasmas, which were formed

and heated by ECRH or one of two tangential neutral beam injectors (NBI). One of them (co-injector, NBI 1) has beam energy $E_{\text{NBI}} = 32 \text{ keV}$ and deposited power $P_{\text{NBI}} \sim 0.6 \text{ MW}$. It is directed along the toroidal magnetic field B_0 . Another one is directed oppositely (counter-injector, NBI 2) and it has beam energy $E_{\text{NBI}} = 29 \text{ keV}$ and deposited power $P_{\text{NBI}} \sim 0.45 \text{ MW}$. The beams have sub-Alfvénic velocity $V_{\text{NBI}} \sim 2.5 \times 10^6 \text{ m} \cdot \text{s}^{-1}$. Line-averaged plasma electron density was low ($\bar{n}_e \sim (0.4 \dots 1.7) \cdot 10^{19} \text{ m}^{-3}$), the center electron temperature was $T_e(0) \sim 1 \dots 2 \text{ keV}$ during ECRH phase and $T_e(0) \sim 0.5 \text{ keV}$ during NBI.

TJ-II is equipped with the Mirnov probe (MP) array placed inside the vacuum vessel for magnetic measurements [7] and the bolometer array for plasma radiation monitoring [8]. Center electron temperature time evolution was obtained from center ECE channel, which was calibrated by the Thomson scattering diagnostic providing n_e and T_e profiles once per shot [9]. For spatial location of the modes we used the advanced dual HIBP diagnostic, consisting from two HIBPs with Cs^+ ions with energies up to 150 keV separated along the torus at 90 degrees.

The HIBP simultaneously provides the information on the local values of plasma electrostatic potential and its oscillations and also electron density and poloidal magnetic field oscillations at the observation point – sample volume (SV). Local plasma potential is proportional to the difference between primary and secondary beam energy:

$$\varphi^{\text{SV}} = \frac{E_{\text{d}} - E_{\text{b}}}{e},$$

where E_{b} is the energy of injected Cs^+ ions and E_{d} is the energy of detected Cs^{++} ions which were ionized at the SV [10].

In low density plasmas ($\bar{n}_e < 1.3 \cdot 10^{19} \text{ m}^{-3}$), when beam attenuation can be neglected, the local plasma density n_e^{SV} is proportional to the secondary beam intensity I_{tot} :

$$I_{tot}(\rho, t) \approx 2I_b n_e^{SV} \sigma^{12} \lambda,$$

where I_b is primary beam current, σ^{12} is the effective cross-sections for electron impact ionization of primary ions, and λ is the length of the SV [5, 10]. So, total current fluctuations are equal to electron density fluctuations δn_e : $\delta I_{tot}(\rho, t)/I_{tot}(\rho) = \delta n_e(\rho, t)$ [10, 11].

The poloidal magnetic field B_{pol} creates the Lorentz force which leads to the appearance of a toroidal velocity component of the beam along the orbit:

$$m \frac{dV}{dt} = Ze[V \times B],$$

here V is the probing particle velocity, m is its mass and B is the total magnetic field. Thus, the poloidal field B_{pol} fluctuations may be retrieved from toroidal velocity V_ζ and shift ζ of the probing beam in the detector using the integral relations [10, 11].

On TJ-II two HIBPs allow conducting unique studies of long-range correlations of the measured plasma parameters. HIBP-I has 2-slit energy analyzer providing 2 neighboring SVs in plasma while HIBP-II has 5-slit analyzer observing 5 SVs. The distance between SVs in plasma is 1...2 cm for HIBP-I and 0.1...0.9 cm for HIBP-II. Both HIBPs can operate in scanning mode, when SV moves from LFS to HFS via plasma center, and in the fixed position mode [12].

2. EXPERIMENTAL RESULTS

2.1. ALFVÉN EIGENMODES

Alfvén eigenmodes (AE) are typically observed in NBI TJ-II discharges. Fig. 1 shows a discharge scenario with HIBP-II scanning and power spectral density (PSD) spectrogram of Mirnov probe signal, showing AE evolution during the discharge. Time intervals from red and yellow rectangles are used to plot PSD spectrograms of plasma potential ϕ , plasma density ($\sim \delta I/I$), poloidal magnetic field ($\sim \zeta$) and HIBP total current vs SV position, ρ , representing plasma electron density profile (Fig. 2). Here ρ is the magnetic flux surface label normalized to the radius of the last closed magnetic surface, $\rho < 0$ indicates the HFS, and $\rho > 0$ – the LFS of the plasma column. Fig. 2 shows that both in NBI1 and NBI2 density fluctuations ($\delta n/n \sim \delta I/I$) at AE frequency are localized at $0.4 < |\rho| < 0.8$. AE associated potential perturbations also show this kind of localization and a pronounced peak at $|\rho| < 0.25$. The same picture is observed on the spectrogram of coherency between plasma potential and MP signal. PSD(ζ) shows a bit different picture: HFS AE peak is present, center peak is much wider than on PSD(ϕ) and LFS peak is absent. This picture may be caused by non-local effects since ζ is an integrated signal.

2.2. SUPRATHERMAL ELECTRON MODES

In low-density ECRH (on-axis heating) plasmas ($\bar{n}_e \sim 0.4 \cdot 10^{19} \text{ m}^{-3}$, $T_e(0) \sim 1 \text{ keV}$) QC modes with $f \sim 20 \text{ kHz}$ are observed at the plasma core $0.2 < |\rho| < 0.6$ (Fig. 3). These modes are not seen on magnetic signals

such as Mirnov probes and ζ but clearly seen on power spectra of AXUV detector and electrostatic HIBP signals. It is supposed that these modes are driven by suprathermal electrons [13].

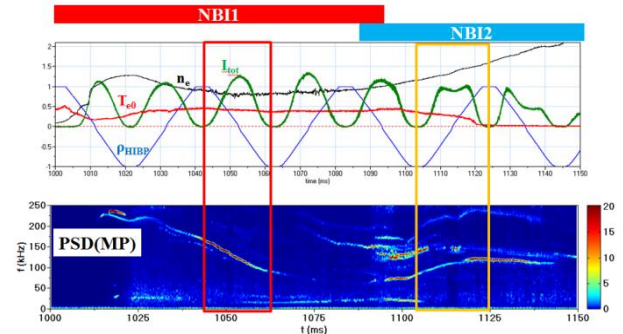


Fig. 1. Plasma scenario (Co-(NBI1) and Counter-(NBI 2) neutral beam injection) with HIBP-II scanning and PSD spectrogram of Mirnov probe signal

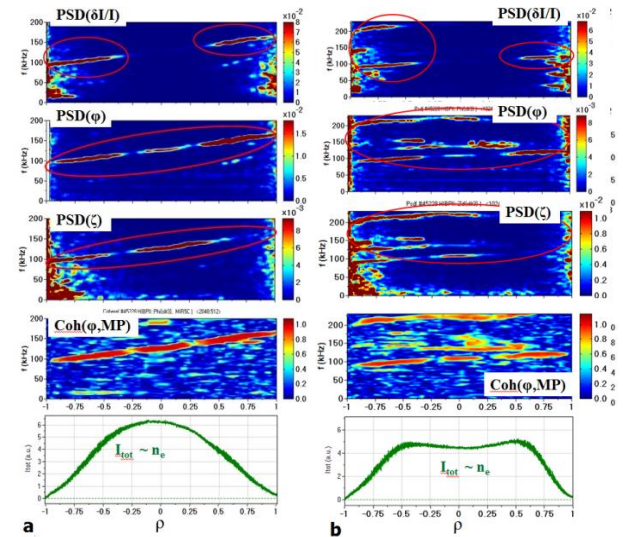


Fig. 2. PSD spectrograms of HIBP-II signals, coherency between ϕ_{HIBP} and MP and HIBP-II total current vs ρ in a) Co-injection (NBI 1), red rectangle in Fig. 2 and b) Counter-injection (NBI 2), yellow rectangle in Fig. 1

2.3. LONG-RANGE CORRELATIONS

Long-Range plasma potential Correlations are observed in low-density ECRH TJ-II plasmas ($\bar{n}_e \sim 0.5 \cdot 10^{19} \text{ m}^{-3}$, $T_e(0) \sim 1.5 \dots 2 \text{ keV}$).

High level of coherency between plasma potentials, measured with HIBP-I and HIBP-II (both beams are concordantly scanning from LFS to HFS), extends from 0 to 30 kHz in radial range $|\rho| < 0.8$ (Fig. 4).

2.4. TEARING-LIKE MODES

Strong low-frequency tearing-like modes ($f_{TLM} \sim 10 \text{ kHz}$) were observed in NBI plasmas ($\bar{n}_e \sim 1.8 \cdot 10^{19} \text{ m}^{-3}$, $T_e(0) \sim 0.4 \text{ keV}$). The mode is clearly seen on both MP signal and HIBP I_{tot} . Raw HIBP total current signal shows the localization of this mode $0.6 < |\rho| < 1$ (Fig. 5). This mode looks similar to the density-resonant MHD modes, observed in [14]. On the contrary there are no any link observed between the mode excitation and specific values of the line-averaged

density. A detailed study of this mode is a topic for further research.

Frequency range and radial location of LRC, ST, AE and TLM modes

Mode type	Frequency range, kHz	Radial range, $ \rho $
LRC, electrostatic	≤ 30	< 0.8
ST, electrostatic	15...25	0.2...0.6
AE, electromagnetic	100...300	0.4...0.8
TLM, magnetic	10...15	0.6...1

CONCLUSIONS

Radial location of various types of quasicohherent modes in TJ-II stellarator was analyzed by dual HIBP. Frequency range and radial location of Long-Range Correlations (LRC), Suprathermal electron mods (ST), Alfvén Eigenmodes (AE) and Tearing-like modes (TLM) are collected in Table.

ACKNOWLEDGEMENTS

Authors are grateful to Drs. M. Ochando and E. Ascasibar for providing the AXUV and Mirnov Probe data. The work of Kurchatov team was supported by Russian Science Foundation (project 14-22-00193). A.V. Melnikov was partly supported by the Competitiveness Program of NRNU MEPhI. The work of Kharkov team was supported by STCU, P-507F.

REFERENCES

1. A.V. Melnikov et al. Heavy ion beam probing – a tool to study geodesic acoustic modes and alfvén eigenmodes in the T-10 tokamak and TJ-II stellarator // *Problems of Atomic Sci. and Technol. Series "Plasma Physics"*. 2017, № 1(23), p. 237.
2. A.V. Melnikov et al. The features of the global GAM in OH and ECRH plasmas in the T-10 tokamak // *Nucl. Fusion*. 2015, v. 55, p. 063001.
3. A.V. Melnikov et al. ECRH effect on the electric potential and turbulence in the TJ-II stellarator and T-10 tokamak plasmas // *Plasma Phys. Control. Fusion*. 2018, v. 60, p. 084008.
4. A.V. Melnikov et al. Study of NBI-driven chirping mode properties and radial location by the heavy ion beam probe in the TJ-II stellarator // *Nucl. Fusion*. 2016, v. 56, p. 112019.
5. A.V. Melnikov et al. Detection and investigation of chirping Alfvén eigenmodes with heavy ion beam probe in the TJ-II stellarator // *Nucl. Fusion*. 2018, v. 58, p. 082019.
6. A.V. Melnikov et al. Effect of magnetic configuration on frequency of NBI-driven Alfvén modes in TJ-II // *Nucl. Fusion*. 2014, v. 54, p. 123002.
7. R. Jiménez-Gómez et al. Alfvén eigenmodes measured in the TJ-II stellarator // *Nucl. Fusion*. 2011, v. 51, p. 033001.
8. M.A. Ochando et al. Up-Down and In-Out Asymmetry Monitoring Based on Broadband Radiation Detectors // *Fusion Sci. Technol.* 2006, v. 50, p. 313.
9. C.J. Barth et al. High-resolution multiposition Thomson scattering for the TJ-II stellarator // *Rev. Sci. Instruments*. 1999, № 1, v. 70, p. 763-767.

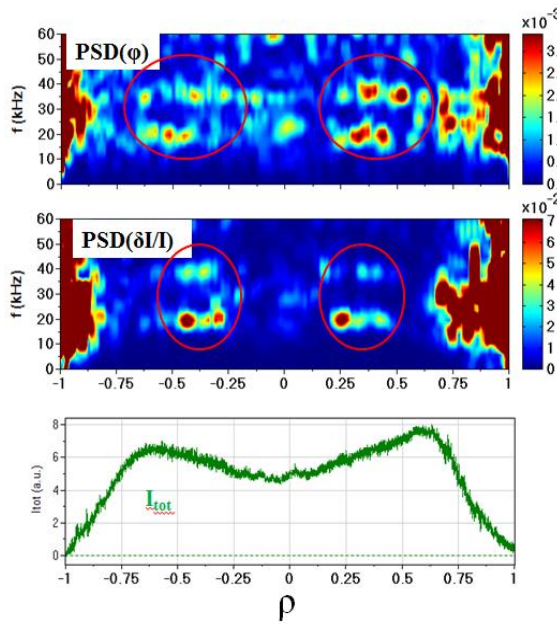


Fig. 3. PSD spectrograms of HIBP-II signals (φ and $\delta I/I$) and HIBP-II total current vs ρ during ECRH, ($\bar{n}_e \sim 0.4 \cdot 10^{19} \text{ m}^{-3}$, $T_e(0) \sim 1 \text{ keV}$)

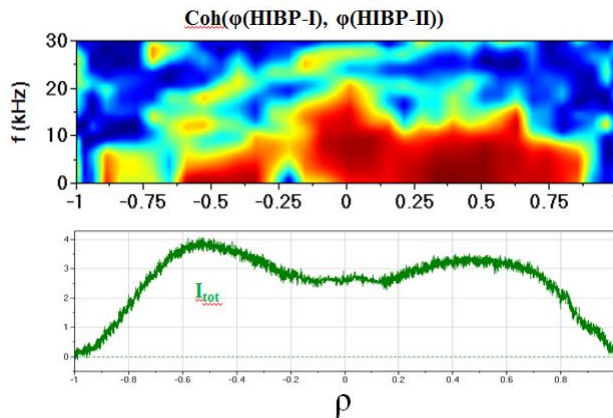


Fig. 4. Spectrogram of coherency between plasma potentials measured by HIBP-I and II (both are scanning) during ECRH, $\bar{n}_e \sim 0.5 \cdot 10^{19} \text{ m}^{-3}$, $T_e(0) \sim 1.5 \dots 2 \text{ keV}$

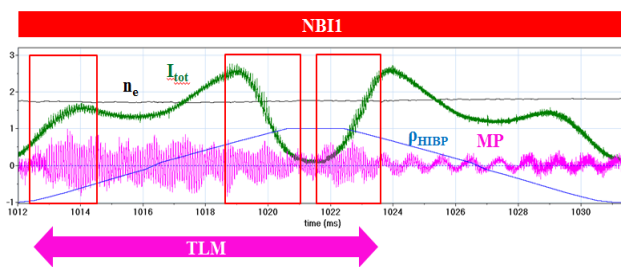


Fig. 5. Tearing-like mode observed during Co-injection of neutral beam (NBI 1), HIBP-II is scanning

10. Yu.N. Dnestrovskij et al. Development of heavy ion beam probe diagnostics // *IEEE Trans. Plasma Sci.* 1994, v. 22, p. 310.
11. A.V. Melnikov et al. Internal measurements of Alfvén eigenmodes with heavy ion beam probing in toroidal plasmas // *Nucl. Fusion.* 2010, v. 50, p. 084023.
12. A.V. Melnikov et al. Heavy ion beam probing – diagnostics to study potential and turbulence in toroidal plasmas // *Nucl. Fusion.* 2017, v. 57, p. 072004.

13. A.V. Melnikov et al. A Quasi-Coherent Electrostatic Mode in ECRH Plasmas on TJ-II // *Plasma and Fusion Research.* 2011, v. 6, p. 2402030.
14. B.Ph. van Milligen et al. A global resonance phenomenon at the TJ-II stellarator // *Nucl. Fusion.* 2011, v. 51, p. 013005.

Article received 20.10.2018

ИССЛЕДОВАНИЕ РАДИАЛЬНОЙ ЛОКАЛИЗАЦИИ КВАЗИКОГЕРЕНТНЫХ МОД С ПОМОЩЬЮ ЗОНДИРОВАНИЯ ПУЧКОМ ТЯЖЕЛЫХ ИОНОВ НА СТЕЛЛАРАТОРЕ TJ-II

Ф.О. Хабанов, Л.Г. Елисеев, Н.К. Харчев, К. Идальго, А.С. Козачек, Л.И. Крупник, С.Е. Лысенко, А.В. Мельников, А.А. Чмыга, Г.Н. Дешко, С.М. Хребтов, А.Д. Комаров, А. Молинеро, Х.Л. де Паблос и команда стелларатора TJ-II

Эксперименты на стеллараторе TJ-II показывают, что альфвеновские моды в частотном диапазоне $100 \text{ кГц} < f_{\text{AE}} < 300 \text{ кГц}$ возбуждаются в режимах с инъекцией пучка нейтральных атомов, а также в режимах с комбинированным ЭЦР-нагревом и нейтральной инъекцией при среднехордовой плотности электронов $n_e = (0,3 \dots 1,5) \times 10^{19} \text{ м}^{-3}$. Моды возбуждаются как на стороне слабого, так и на стороне сильного поля. Кроме того, в плазме TJ-II наблюдаются моды с частотами $f < 30 \text{ кГц}$, а именно моды, возбуждаемые быстрыми электронами, тиринг-подобные моды, а также моды, характеризующиеся дальними корреляциями электрического потенциала. Некоторые моды имеют только электростатическую компоненту колебаний, другие также видны на спектрах колебаний плотности электронов и полоидального магнитного поля. В рамках данной работы была определена радиальная локализация каждого типа упомянутых квазикогерентных мод. Для этого использовались два диагностических комплекса на пучках тяжелых ионов, магнитные зонды и болометры (AXUV-детекторы).

ДОСЛІДЖЕННЯ РАДІАЛЬНОЇ ЛОКАЛІЗАЦІЇ КВАЗІКОГЕРЕНТНИХ МОД ЗА ДОПОМОГОЮ ЗОНДУВАННЯ ПУЧКОМ ВАЖКИХ ІОНІВ НА СТЕЛАРАТОРІ TJ-II

Ф.О. Хабанов, Л.Г. Єлісеєв, М.К. Харчев, К. Ідальго, О.С. Козачок, Л.І. Крупник, С.Є. Лисенко, О.В. Мельніков, О.О. Чмига, Г.М. Дешко, С.М. Хребтов, О.Д. Комаров, А. Молинеро, Х.Л. де Паблос та команда стелларатора TJ-II

Експерименти на стеллараторі TJ-II показують, що альфвеновські моды у частотному діапазоні $100 \text{ кГц} < f_{\text{AE}} < 300 \text{ кГц}$ збуджуються в режимах з інжекцією пучка нейтральних атомів, а також в режимах з комбінованим ЕЦР-нагріванням і нейтральною інжекцією при середньохордовій густині електронів $n_e = (0,3 \dots 1,5) \times 10^{19} \text{ м}^{-3}$. Моды збуджуються як на стороні слабого, так і на стороні сильного поля. Крім того, у плазмі TJ-II спостерігаються моды з частотами $f < 30 \text{ кГц}$, а саме моды, що збуджуються швидкими електронами, тірінг-подібні моды, а також моды, що характеризуються далекими кореляціями електричного потенціалу. Деякі моды мають тільки електростатичну компоненту коливань, інші також видно на спектрах коливань густини електронів і полоїдального магнітного поля. У рамках даної роботи була визначена радіальна локалізація кожного типу згаданих квазікогерентних мод. Для цього використовувалися два діагностичних комплекси на пучках важких іонів, магнітні зонди і болометри (AXUV-детектори).